



The role of aromatic precursors in the formation of haloacetamides by chloramination of dissolved organic matter



Julien Le Roux^{a, b}, Maolida Nihemaiti^{a, c}, Jean-Philippe Croué^{a, c, *}

^a Water Desalination and Reuse Center, 4700 KAUST, Thuwal 23955-6900, Saudi Arabia

^b LEESU (UMR MA 102), Université Paris-Est - AgroParisTech, 61 avenue du Général de Gaulle, 94010 Créteil cedex, France

^c Curtin Water Quality Research Centre, Department of Chemistry, Curtin University, GPO Box U1987, Perth, WA 6845, Australia

ARTICLE INFO

Article history:

Received 28 July 2015

Received in revised form

16 October 2015

Accepted 18 October 2015

Available online 21 October 2015

Keywords:

Chloramination

Disinfection byproducts

Haloacetamides

Dissolved organic matter

Aromatic compounds

ABSTRACT

Water treatment utilities are diversifying their water sources and often rely on waters enriched in nitrogen-containing compounds (e.g., ammonia, organic nitrogen such as amino acids). The disinfection of waters exhibiting high levels of nitrogen has been associated with the formation of nitrogenous disinfection byproducts (N-DBPs) such as haloacetonitriles (HANs) and haloacetamides (HAcAms). While the potential precursors of HANs have been extensively studied, only few investigations are available regarding the nature of HAcAm precursors. Previous research has suggested that HAcAms are hydrolysis products of HANs. Nevertheless, it has been recently suggested that HAcAms can be formed independently, especially during chloramination of humic substances. When used as a disinfectant, monochloramine can also be a source of nitrogen for N-DBPs. This study investigated the role of aromatic organic matter in the formation of N-DBPs (HAcAms and HANs) upon chloramination. Formation kinetics were performed from various fractions of organic matter isolated from surface waters or treated wastewater effluents. Experiments were conducted with ¹⁵N-labeled monochloramine (¹⁵NH₂Cl) to trace the origin of nitrogen. N-DBP formation showed a two-step profile: (1) a rapid formation following second-order reaction kinetics and incorporating nitrogen atom originating from the organic matrix (e.g., amine groups); and (2) a slower and linear increase correlated with exposure to chloramines, incorporating inorganic nitrogen (¹⁵N) from ¹⁵NH₂Cl into aromatic moieties. Organic matter isolates showing high aromatic character (i.e., high SUVA) exhibited high reactivity characterized by a major incorporation of ¹⁵N in N-DBPs. A significantly lower incorporation was observed for low-aromatic-content organic matter. ¹⁵N-DCAcAm and ¹⁵N-DCAN formations exhibited a linear correlation, suggesting a similar behavior of ¹⁵N incorporation as SUVA increases. Chloramination of aromatic model compounds (i.e., phenol and resorcinol) showed higher HAcAm and HAN formation potentials than nitrogenous precursors (i.e., amino acids) usually considered as main precursors of these N-DBPs. These results demonstrate the importance of aromatic organic compounds in the formation of N-DBPs, which is of significant importance for water treatment facilities using chloramines as final disinfectant.

© 2015 Elsevier Ltd. All rights reserved.

1. Introduction

Surface waters are often impacted by human activities (e.g., agriculture, industries, and municipal wastewater effluent discharges) resulting in their enrichment in nitrogen-containing compounds (i.e., ammonia and organic nitrogen such as amino

acids) (Westerhoff and Mash, 2002). The disinfection of waters exhibiting high levels of nitrogen has been associated with the formation of nitrogenous disinfection byproducts (N-DBPs) (Bond et al., 2011). N-DBPs generally form in significantly lower concentrations than regulated DBPs, but have been a growing concern over the past decade because of their higher health risk (Muellner et al., 2007; Plewa et al., 2004). *In vitro* mammalian cell tests have demonstrated that haloacetonitriles (HANs), halonitromethanes (HNMs), and haloacetamides (HAcAms) are more cytotoxic and genotoxic (i.e., up to 2 orders of magnitude) than non-nitrogenous molecules such as trihalomethanes (THMs) and haloacetic acids

* Corresponding author. Curtin Water Quality Research Centre, Department of Chemistry, Curtin University, GPO Box U1987, Perth, WA 6845, Australia.

E-mail addresses: julien.le-roux@u-pec.fr (J. Le Roux), maolida.nihemaiti@postgrad.curtin.edu.au (M. Nihemaiti), jean-philippe.croue@curtin.edu.au (J.-P. Croué).

(HAAs) (Plewa et al., 2008). Nitrogen in N-DBPs can also be derived from chloramines when used as disinfectants. Water utilities have been increasingly switching to monochloramine as an alternative to chlorine in order to limit the production of regulated THMs and HAAs. Nevertheless, concern has been raised regarding the formation of N-DBPs (e.g., N-nitrosodimethylamine – NDMA) produced from the reaction between monochloramine and secondary or tertiary amines (Mitch and Sedlak, 2004).

Among N-DBPs, dichloroacetonitrile (DCAN) and dichloroacetamide (DCAcAm) are the most frequently detected species in drinking water treatment plants (Krasner et al., 2006). While the potential precursors of HANs have been extensively studied, only few investigations are available regarding the nature of HACams precursors. HACams were first reported to be intermediate products of HANs hydrolysis and ultimately decomposed to HAAs (Glezer et al., 1999; Reckhow et al., 2001). More recently, it was found that HACams can be formed independently from HANs during chlorination and chloramination processes (Huang et al., 2012). Two different pathways have been proposed to describe the formation of HANs and HACams (Fig. S1). First, the Decarboxylation Pathway occurs by rapid chlorination or chloramination of α -amine groups of free amino acids to form a nitrile, followed by hydrolysis to release HANs and carbonic acid (Trehly et al., 1986). HANs are then further hydrolyzed to HACams and HAAs (Reckhow et al., 2001). The second pathway proposed for HANs formation is the Aldehyde Pathway, where nitrogen from monochloramine (NH_2Cl) is incorporated into aldehydes to produce nitriles. The reaction between NH_2Cl and formaldehyde forms cyanogen chloride (CNCl) (Pedersen et al., 1999), and chloroacetonitrile is formed from chloroacetaldehyde (Kimura et al., 2013). Haloacetaldehydes (HACAls) are carbonaceous DBPs frequently detected in disinfected waters, and often represent the third major class of DBPs after THMs and HAAs (Krasner et al., 2006). Chloroacetaldehyde has been demonstrated to be a precursor of N,2-dichloroacetamide upon chloramination (Kimura et al., 2013). The reaction involves the incorporation of the nitrogen atom of monochloramine (NH_2Cl) to form the amide group through the formation of a carbinolamine intermediate.

In addition to the Aldehyde Pathway, most studies about HANs and HACams formation mechanisms focused on the chlorination of nitrogenous precursors (e.g., amino acids, amines, pyrimidines) or matrices enriched in nitrogenous moieties (e.g., algae cells, extracellular organic matter) (Bond et al., 2009; Fang et al., 2010; Oliver, 1983; Reckhow et al., 2001; Yang et al., 2010, 2011, 2012). In the case of aquatic humic substances, a positive correlation was found between their nitrogen content and their tendency to form HAN upon chlorination (Reckhow et al., 1990). Studies performed with labeled ^{15}N -chloramines ($^{15}\text{NH}_2\text{Cl}$) on nitrogenous organic (N-org) precursors and fractions of dissolved organic matter (DOM) found that nitrogen in HANs or CNCl originated from both organic precursors and NH_2Cl (Yang et al., 2010). Recent studies suggested that aromatic moieties of DOM may contribute to a substantial HAN formation upon chloramination (Chuang et al., 2013; Huang et al., 2012; Yang et al., 2008, 2010). During chloramination, the formation of DCAN or CNCl did not correlate with the DON/DOC ratios of DOM fractions. However, good correlations were observed with their SUVA values and thus with their aromatic carbon content (Yang et al., 2008). A mechanism describing the chloramination of a β -diketone moiety was proposed based on the Decarboxylation Pathway, showing the incorporation of nitrogen through the formation of an N-chloroimine and leading to DCAN as a hydrolysis product. Approximately 90% of nitrogen in DCAN and CNCl was reported to originate from NH_2Cl reaction with Suwannee River DOM (Yang et al., 2010). Recent kinetics experiments also suggest similarities between HANs, THMs, and HAAs precursors (Chuang

et al., 2013). Kinetics of DCAN and trichloronitromethane (TCNM) formation upon chloramination using $^{15}\text{NH}_2\text{Cl}$ were proposed to involve two reaction mechanisms: formation from N-org precursors following a second-order reaction; and formation by incorporation of nitrogen from NH_2Cl , linearly correlated with chloramines exposure (Chuang and Tung, 2015).

Less information is available about HACams precursors and formation mechanisms, since HACams were first reported as DBPs in a 2000–2002 drinking water survey (Krasner et al., 2006; Weinberg et al., 2002). Although DCAcAm yields from amino acids are considerably lower than those of DCAN, comparable levels (i.e., median concentrations of 1.3 and 1 $\mu\text{g/L}$, respectively) have been observed in US drinking waters (Bond et al., 2012; Krasner et al., 2006). Therefore, unknown precursors appear to be responsible for the majority of HACam formation (Bond et al., 2012). The formation of HACams from algal exopolymeric substances (EPS), municipal wastewater treatment plant effluents (Huang et al., 2012), natural waters (Chu et al., 2013), bacterial cells (Huang et al., 2013), natural organic matter (NOM) fractions, and free amino acids (Chu et al., 2010a, 2010b) has been previously studied. The hydrophilic acid fraction isolated from an algal-impacted water enriched in nitrogen (i.e., high DON/DOC ratio), exhibited the highest DCAcAm formation potential during both chlorination and chloramination, which was associated with the presence of protein-like organic matter (Chu et al., 2010b). However, DCAcAm was recently found to be preferentially formed by chloramination of humic materials, while chlorination of wastewater effluents and algal EPS tended to form more DCAN (Huang et al., 2012). These results suggested that the mechanism of HACams formation is independent from that of HANs. Overall, HACams formation mechanisms remain unclear, and the precursors of HACams in natural waters still need to be characterized.

This study investigated the role of aromatic organic matter in the formation of N-DBPs (i.e., especially HACams) upon chloramination, with emphasis on the formation kinetics of HACams and HANs. Various fractions of organic matter isolated from different waters (i.e., surface waters, treated wastewater) as well as model compounds were studied to understand the factors controlling N-DBPs formation. Experiments were conducted with $^{15}\text{NH}_2\text{Cl}$ to trace the origin of nitrogen in the formed DBPs.

2. Materials and methods

2.1. Materials

All reagents were of analytical or laboratory grade and were used without further purification. MilliQ water was produced with a Millipore system (18.2 M Ω cm). Sodium hypochlorite (NaOCl, 5.65–6%, Fisher Scientific) and ammonium chloride (Acros Organics, 99.6%) were used to prepare chloramine reagents. ^{15}N -labeled ammonium chloride was purchased from Sigma–Aldrich (98%). Sodium thiosulfate (Fisher Scientific) was used to quench residual chloramines. Methyl tert-butyl ether (MTBE) and ethyl acetate (>99%, Fisher Scientific) were used for DBP extractions without further purification. A THM calibration mix (chloroform – TCM, dichlorobromomethane – CHCl_2Br , chlorodibromomethane – CHClBr_2 , and bromoform – TBM), a mixed standard (EPA 551B Halogenated Volatiles Mix) containing haloacetonitriles (HANs), trichloronitromethane (TCNM, or chloropicrin) and haloketones (HKs), and a mixed standard containing 9 HAAs (EPA 552.2 Methyl Ester Calibration Mix) were supplied from Supelco (Sigma–Aldrich). Chloro-, bromo-, dichloro-, and trichloroacetamide were obtained from Sigma–Aldrich. Other haloacetamides (HACams) were purchased from Cansyn Chem. Corp. Decafluorobiphenyl (99%, Sigma–Aldrich, Supelco) was used as a surrogate standard. 2-

bromopropionic acid (Fluka Analytical) was used as a surrogate for HAA extractions and analyses. Phenol (>99%), resorcinol (>99%), L-tyrosine (>98%), L-aspartic acid (>99.5%) and L-tryptophan (>98%) were obtained from Sigma–Aldrich.

2.2. Experimental methods

All glassware used during these experiments was washed with Milli-Q water and baked at 500 °C for at least 5 h prior to use. DOM stock solutions were prepared by dissolving 20 mg of a selected DOM isolate in 500 mL of Milli-Q water (dissolved organic carbon, i.e., DOC ~ 14–19 mg C/L). Solutions for experimentation were prepared by adjusting DOC to 5 mg C/L in 10 mM phosphate buffer. Monochloramine and ¹⁵N-labeled monochloramine stock solutions were prepared by adding sodium hypochlorite (NaOCl) to a continuously-stirred ammonium chloride or ¹⁵N-labeled ammonium chloride solution, respectively, adjusted to pH 8.5 with sodium hydroxide, at a N:Cl molar ratio of 1.2:1. The concentration of monochloramine stock solutions was adjusted to a desired concentration. Chloramination experiments were performed in headspace-free 65 mL amber glass bottles under excess of disinfectant dosage. The doses were calculated as: $\text{NH}_2\text{Cl (mg/L as Cl}_2) = 3 \times \text{DOC (mg C/L)}$, to conduct a comprehensive comparison between our DBPFP data and results obtained from other studies working with similar doses (Chu et al., 2010b; Dotson et al., 2009; Krasner et al., 2007). Monochloramine was also added in excess for the determination of DBPFP of model organic compounds (i.e., phenol, resorcinol, tyrosine, aspartic acid, and tryptophan) solutions (chloramine/model compound molar ratio = 5.6). Most of the experiments were conducted in duplicates, at room temperature (22 ± 1 °C), and under dark conditions to avoid any photolysis reaction. At the end of the reaction time, chlorine residual was quenched using a slight excess of sodium thiosulfate. To avoid any loss of the targeted by-products, samples were extracted immediately after quenching. Free chlorine and total chlorine concentrations in the stock solutions of sodium hypochlorite were determined iodometrically with sodium thiosulfate 0.1 M (>99.9%). Initial NH_2Cl and NHCl_2 concentrations were determined by spectrophotometric measurement using their respective molar extinction coefficients at 245 nm and 295 nm and by solving simultaneous equations (Schreiber and Mitch, 2005). Residual oxidant was analyzed iodometrically (Eaton et al., 1995). Oxidant exposures were calculated based upon the integration of concentration versus time curves of oxidant decay.

2.3. Analytical methods

Total Organic Carbon (TOC) and Total Nitrogen (TN) concentrations were measured using a TOC analyzer equipped with a TN detection unit (TOC-VCSH, Shimadzu). UV_{254} absorbance was measured using UV–Vis spectrometer (UV-2550, Shimadzu) and specific UV absorbance at 254 nm (SUVA) values were calculated as $\text{UV}_{254}/\text{DOC}$ ratio and expressed as $\text{L.mg}^{-1}.\text{m}^{-1}$. Four trihalomethanes (THMs), four haloacetonitriles (HANs), two haloacetones (HKs), and chloropicrin were extracted and analyzed following EPA method 551, which consists of a liquid–liquid extraction using MTBE followed by gas chromatography coupled with electron capture detector (GC-ECD) or mass spectrometer (GC–MS) (Munch and Hautman, 1995). Nine HAAs were extracted and analyzed following EPA method 552.2, which is based on a liquid–liquid extraction with MTBE in acidic conditions followed by derivatization to methyl esters using acidic methanol, and analysis by gas chromatography coupled with mass spectrometry (GC–MS) (Munch and Munch, 1995). HAAs were analyzed following the same EPA method 551 protocol, replacing MTBE by ethyl acetate for

the liquid–liquid extraction. For experiments involving ¹⁵N– NH_2Cl , all extracts were analyzed by GC–MS. Since ¹⁵N-labeled DBPs (¹⁵N-DBPs) are not commercially available, the concentration of ¹⁵N-DBPs was quantified indirectly using the concentration of unlabeled DBPs (i.e., ¹⁴N-DBPs), based on the assumption that the MS response for ¹⁴N-DBPs is similar to that for ¹⁵N-DBPs (Huang et al., 2012). As an example, DCAN concentrations were determined using m/z 74 and 75 as quantification ions for ¹⁴N-DCAN and ¹⁵N-DCAN, respectively, and using the calibration curve obtained from ¹⁴N-DCAN standards. The same method was used for other ¹⁵N-DBPs analysis. Additional analytical details and the list of labeled and unlabeled DBPs and their related quantification ions are provided in Text S1 and Table S1 (SI).

2.4. Characteristics of DOM extracts

Samples of wastewater were collected at the Jeddah wastewater (JW) treatment plant (Saudi Arabia) in September 2012 and stored at 4 °C prior to the extraction. The hydrophobic (JW HPO), transphilic (JW TPI), and colloidal (JW COL) effluent organic matter (EfOM) fractions were obtained from these samples. Three previously isolated hydrophobic NOM fractions (i.e., hydrophobic acids-HPOA obtained from base desorption, and hydrophobic-HPO isolated with acetonitrile/water desorption) showing different chemical composition were selected: SR HPOA isolated from the Suwannee River (Georgia, USA), BR HPO isolated from the Blavet River (Côte d'Armor, France), and GR HPO obtained from the Gartempe River (Vienne, France). One hydrophilic acid (RR HPI) isolated from the Ribou River (Maine-et-Loire, France) was also selected. NOM fractions were isolated using two slightly different comprehensive isolation protocols described elsewhere (Croué, 2004; Leenheer et al., 2000). All fractions and their chemical compositions are described in Table S2 (SI).

3. Results and discussion

3.1. Kinetics of DBP formation

In preliminary experiments, the kinetics of DBPs formation were assessed during chloramination over 72 h on EfOM isolates (JW HPO and JW TPI) and Suwannee River NOM (SR HPOA). Monochloramine concentration remained in excess during all the reaction time (Fig. S2, SI). The decay of monochloramine was always caused by its autodecomposition since no significant variations were observed between all the experiments, and the experimental values fitted well with the autodecomposition model reported by Jafvert and Valentine (1992).

DCAcAm formation from the three isolates (SR HPOA, JW HPO, JW TPI) showed a two steps profile: a rapid formation in the first 3 h of reaction, followed by a linear increase (Fig. 1a). The formation of DCAcAm from JW TPI increased slightly faster than from JW HPO during the first 24 h of reaction, and then slowed down between 24 h and 72 h. A linear increase was observed for JW HPO, finally reaching a concentration similar to that of JW TPI at 72 h of reaction (42.9 nM and 38.6 nM for JW HPO and JW TPI, respectively). This finding indicates that the nature of EfOM precursors (as described by their C/N ratio and hydrophobicity in terms of SUVA values, see Table S2, SI) might play an important role in formation kinetics, but exerts a lesser influence on the overall formation potential. A lower concentration of nitrogenous precursors in JW HPO (i.e., as revealed by its higher C/N ratio of 19.5, compared to 8.4 for JW TPI, Table S2, SI) could lead to a lower formation of DCAcAm in the first 24 h of reaction, then slow incorporation of nitrogen from monochloramine into the organic matrix would occur with time, leading to a continuous increase in DCAcAm. DCAcAm formation kinetics from

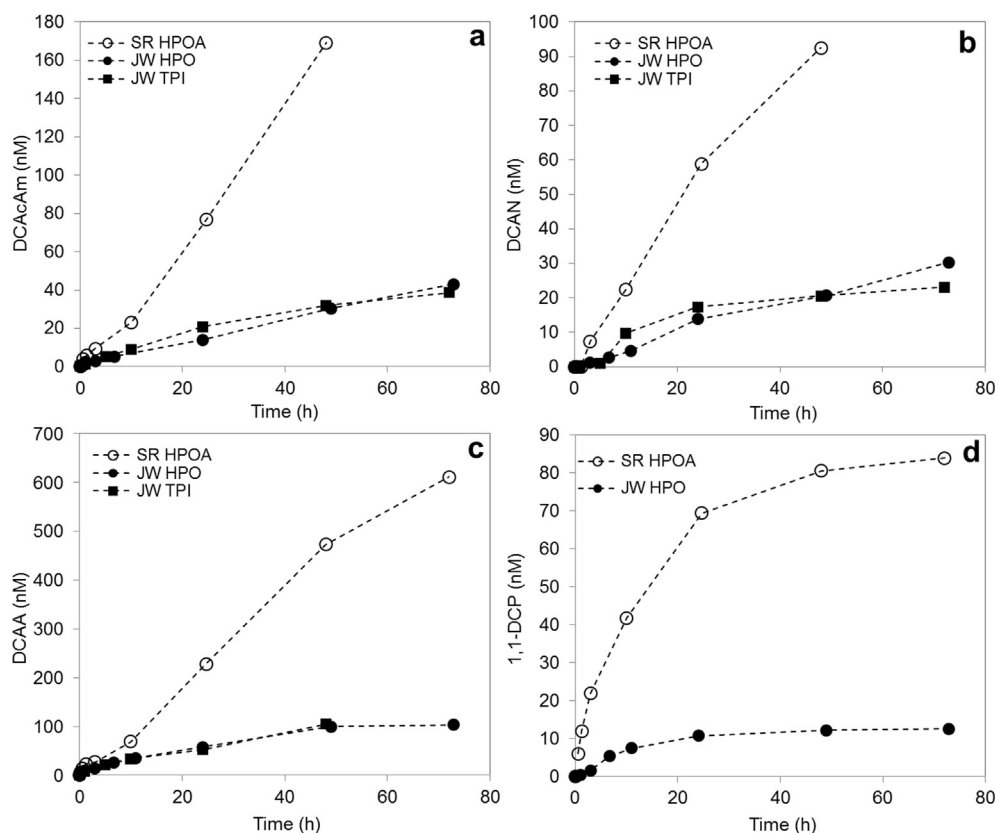


Fig. 1. Formation kinetics of a) DCaAm, b) DCAN, c) DCAA, and d) 1,1-DCP by chloramination (15 mg Cl_2/L) of SR HPOA, JW HPO, and JW TPI isolates (5 mg C/L) at pH 8 (10 mM phosphate buffer).

SR HPOA was significantly faster than that from EfOM isolates. DCaAm concentration quickly increased in the first 10 h of reaction, and then linearly increased even faster after 10 h to reach a final concentration of 169.2 nM (21.7 $\mu\text{g/L}$) at 48 h. The high reactivity of SR HPOA isolate can be related to its aromatic character (i.e., SUVA value = 4.6). High SUVA NOM isolates are generally characterized by a low incorporation of nitrogenous moieties, i.e., high C/N ratio (e.g., C/N ratio of 68.6 for SR HPOA) as compared to other isolates (Table S2, SI) (Leenheer and Croué, 2003). In addition, the substantial difference between SR HPOA and JW HPO reactivities can be explained by their different origins. Especially, EfOM and NOM exhibit different relationships between SUVA and the aromatic carbon content, which is explained by a different origin of aromatic moieties (Drewes and Croué, 2002). Furthermore, EfOM contains less high molecular weight compounds, less compounds with CHO formulae but much more organosulfur compounds with CHOS formulae (e.g., surfactants) as compared to NOM (Gonsior et al., 2011).

DCaAm concentrations from the three isolates did not stabilize after 72 h, thus indicating that precursors were still available in the solutions. No TCaAm was detected (detection limit of 4 nM) from any isolate in the experimental conditions used (i.e., NH_2Cl = 15 mg Cl_2/L and Cl:N ratio of 1:1.2). No brominated HAcAms were detected since no bromide was present in the reaction solutions.

DCAN formation from the three isolates followed similar profiles compared to those of DCaAm formation (Fig. 1b). The difference between JW HPO and JW TPI isolates was even more pronounced: a faster reactivity was observed for JW TPI between 0 and 24 h of reaction, but it slowed down to reach a final concentration of 23.1 nM after 72 h. JW HPO profile showed a progressive increase with time, to finally reach a higher concentration (i.e., 30.3 nM)

than that of JW TPI. As discussed for DCaAm results, the different nature of DBP precursors present in the two JW EfOM isolates (i.e., different proportion of aromatic and nitrogenous precursors), may influence the reaction kinetics. DCAN formation from SR HPOA was also considerably more important than from JW EfOM isolates and increased faster, reaching 92.5 nM after only 48 h. No other HAN was detected from any of the three isolates.

DCAA was the major DBP detected during these experiments, with concentrations of 611.0 nM and 103.1 nM formed after 72 h for SR HPOA and JW HPO, respectively. The SR HPOA isolate was the strongest DCAA precursor with a kinetics profile similar to that of DCaAm. A similar DCAA formation was observed for the two JW EfOM isolates indicating that, unlike N-DBPs, DCAA precursors might be more similar in the two fractions. TCAA was only detected at very low concentrations (<0.005 nM, i.e., <0.8 $\mu\text{g/L}$) for SR HPOA and JW TPI.

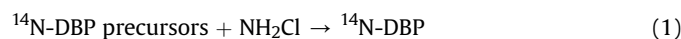
TCM was only detected for SR HPOA, reaching a concentration of 453.1 nM after 72 h. 1,1-dichloropropanone (1,1-DCP) was solely detected during the chloramination of SR HPOA and JW HPO. This observation could be related to the higher proportion of aromatic precursors in these isolates. The formation of HKs has been previously reported from chlorination and chloramination of Black Lake fulvic acids and a Suwannee River reverse osmosis NOM isolate (Reckhow and Singer, 1985; Yang et al., 2007). 1,1-DCP formation rates from both isolates quickly increased in the first 24 h of reaction, but decreased after 24 h to reach final concentrations (at 72 h) of 84.0 nM and 12.6 nM for SR HPOA and JW HPO, respectively. HKs are known as intermediates in the haloform reaction, hydrolyzing to chloroform in neutral and alkaline conditions (Suffet et al., 1976). The formation of HKs has been associated with a higher methyl ketone content in fulvic acids fractions as compared to humic acids

(Reckhow et al., 1990). In our experiments, no 1,1,1-TCP could be detected from any isolate. 1,1,1-TCP can be formed by chlorine attack of 1,1-DCP during chlorination but not during chloramination, because monochloramine is not able to provide further chlorine substitution (Yang et al., 2007).

3.2. Tracing the origin of nitrogen in N-DBPs

To examine the behavior of nitrogen incorporation from organic precursors and NH_2Cl , kinetic experiments were performed with SR HPOA, JW HPO, JW TPI, JW COL, and RR HPI isolates (5 mg C/L) using ^{15}N -labeled monochloramine ($^{15}\text{NH}_2\text{Cl}$) (15 mg/L as Cl_2). DBP formation kinetics in the presence of $^{15}\text{NH}_2\text{Cl}$ exhibited similar profiles than those obtained using $^{14}\text{NH}_2\text{Cl}$. As depicted on Fig. S3 and S4 (SI) for each DOM isolate, the initial fast reaction occurring before 24 h was generally related to the incorporation of ^{14}N from N-org precursors into DCACAm and DCAN. This result is in accordance with the faster reactivity of JW TPI observed in the first 24 h of reaction (Fig. 1) as compared to JW HPO which can be attributed to its higher nitrogen content (i.e., lower C/N ratio). Overall, the isolates exhibited a slow and linear formation of ^{15}N -DCACAm and ^{15}N -DCAN, while the formation of ^{14}N -DCACAm and ^{14}N -DCAN tended to reach a plateau during the 72-h reaction time. For SR HPOA, showing very low nitrogen content, the incorporation of inorganic nitrogen from NH_2Cl was the predominant mechanism after 10 h of reaction (e.g., 84.6% of the DCACAm formed at 48 h was ^{15}N -DCACAm), which explains the steep linear kinetics profiles obtained for DCAN and DCACAm in the preliminary experiments. JW HPO profiles were similar to those of SR HPOA, showing proportions of ^{15}N -DCACAm and ^{15}N -DCAN at 72 h of 74.6% and 68.5%, respectively, which also explains the linearity of profiles shown in Fig. 1. In contrast, the formation of N-DBPs from the JW TPI isolate was more influenced by both mechanisms at the same time (e.g., the proportion of ^{15}N -DCACAm was $49\% \pm 10\%$ throughout the reaction time) thus explaining the non-linear profiles obtained. In the case of the RR HPI isolate, the formation of ^{15}N -DCACAm was slower than that of ^{14}N -DCACAm in the first 40 h of reaction but finally reached a similar concentration after 48 h (i.e., 20.3 nM and 18.3 nM, respectively).

A recent study demonstrated that formation kinetics of N-DBPs (DCAN and TCNM) during chloramination are influenced by two contributions: second-order reaction kinetics from N-org precursors and the incorporation of inorganic nitrogen from chloramines, linearly correlated with chloramines exposure (Chuang and Tung, 2015). Second-order reaction kinetics for ^{14}N -DBP depends on the concentrations of NH_2Cl and ^{14}N -DBP precursors, and can be expressed as Eq. (1):



$$\frac{d[^{14}\text{NDBP}]}{dt} = k[^{14}\text{NDBP precursors}][\text{NH}_2\text{Cl}],$$

where k is the second-order rate constant for the formation of ^{14}N -DBPs. Integrating Eq. (1) for t yields Eq. (2) (Text S2, SI).

$$\begin{aligned} & \frac{1}{([\text{NH}_2\text{Cl}]_i - [^{14}\text{NDBP precursors}]_{\text{Total}})} \\ & \times \ln \left(\frac{[^{14}\text{NDBP precursors}]_{\text{Total}} \times [\text{NH}_2\text{Cl}]}{[\text{NH}_2\text{Cl}]_i \times ([^{14}\text{NDBP precursors}]_{\text{Total}} - [^{14}\text{NDBP}])} \right) \\ & = kt \end{aligned} \quad (2)$$

where $[\text{NH}_2\text{Cl}]_i$ is the initial monochloramine concentration and

$[^{14}\text{N-DBP precursors}]_{\text{Total}}$ is the total ^{14}N -DBP precursors concentration, i.e., the concentration of ^{14}N -DBP formed at 72 h.

Fig. 2 shows the formation of ^{14}N -DCACAm and ^{14}N -DCAN and their respective second-order relationships derived from Eq. (2). Linear relationships were obtained from this second-order model for the formation of the two ^{14}N -DBPs with most of the investigated isolates. The linearity observed for the first 48 h suggests that the reaction was nearly completed after 72 h. This finding confirms that ^{14}N -DBPs produced after 72 h can be used to reflect the total concentration of ^{14}N -DBP precursors. ^{14}N -DCACAm formation followed second-order kinetics for all the isolates. Because JW TPI exhibited a decreasing profile after 24 h and not enough data points were obtained for JW COL, second-order relationships could not be plotted for ^{14}N -DCAN formation from these two isolates. The SR HPOA isolate exhibited the highest formation of ^{14}N -DCACAm (i.e., 28.0 nM), followed by RR HPI, JW TPI, JW HPO, and finally JW COL. A similar order was obtained for the formation of ^{14}N -DCAN, however, JW TPI showed a slight decrease in concentration after 24 h of reaction time, reaching a lower value than JW HPO at 72 h. Because SR HPOA is characterized by the highest C/N ratio (i.e., lowest nitrogenous moieties content) of the studied isolates, these results indicate that there is no direct correlation between nitrogen content of DOM and the production of ^{14}N -DCACAm or ^{14}N -DCAN. Hence, the reactivity of specific organic nitrogen sites plays a more important role in SR HPOA as compared to other fractions of DOM. The aromatic character does not seem to be a critical parameter in the formation of ^{14}N -DBPs, since low SUVA isolates (e.g., RR HPI) exhibited higher formation of ^{14}N -DCACAm and ^{14}N -DCAN than higher SUVA isolates (e.g., JW HPO).

As proposed in the literature (Chuang and Tung, 2015), a linear correlation was observed between ^{15}N -DCAN formation and monochloramine exposure for all isolates investigated (Fig. 3). The same linear correlation was observed for the formation of ^{15}N -DCACAm. SR HPOA exhibited again the highest reactivity, with concentrations of up to 143.2 nM of ^{15}N -DCACAm and 73.4 nM of ^{15}N -DCAN formed after 48 h (i.e., an exposure of 33,922 mg.min/L). In general, isolates with higher SUVA values exhibited more pronounced slopes, which indicates that a major incorporation of ^{15}N occurs during $^{15}\text{NH}_2\text{Cl}$ reaction with organic matter enriched in aromatic moieties. RR HPI formed the highest proportion of ^{14}N -DCACAm (i.e., 47.4% at 48 h) as compared to ^{15}N -DCACAm. The comparison was even more significant for DCAN, with a relative abundance of 72.1% of ^{14}N -DCAN at 48 h, indicating that hydrophilic fractions of DOM enriched in nitrogen (see C/N ratios in Table S2, SI) incorporate a higher proportion of nitrogen from N-org precursors into N-DBPs.

These results explain the N-DBP formation profiles obtained in the experiments involving only $^{14}\text{NH}_2\text{Cl}$ (Fig. 1). The first step of rapid N-DBP production is related to the reactivity of N-org precursors with chlorine atoms of NH_2Cl . As N-org precursors (i.e., ^{14}N -DBP precursors) are consumed, the formation of ^{14}N -DBP tends to stabilize as described by the second-order reaction kinetics. Then, the contribution of non-nitrogenous precursors starts to be significant, exhibiting a slower reactivity with NH_2Cl but finally reaching high N-DBP concentrations. These high concentrations may be due to the higher initial concentrations of non-nitrogenous precursors, i.e., aromatic precursors, as compared to N-org precursors. The second step of linear increase with increasing exposure can thus be described as the slow incorporation of nitrogen from NH_2Cl into non-nitrogenous precursors comprising aromatic moieties.

Aldehydes are known to be precursors of nitriles, and it has been demonstrated that chloroacetaldehyde forms chloroacetamide and N,2-dichloroacetamide (first time identified) in alkaline chloramination conditions (Kimura et al., 2013). HACams can thus be expected to be formed from haloacetaldehydes (HACAl) either directly

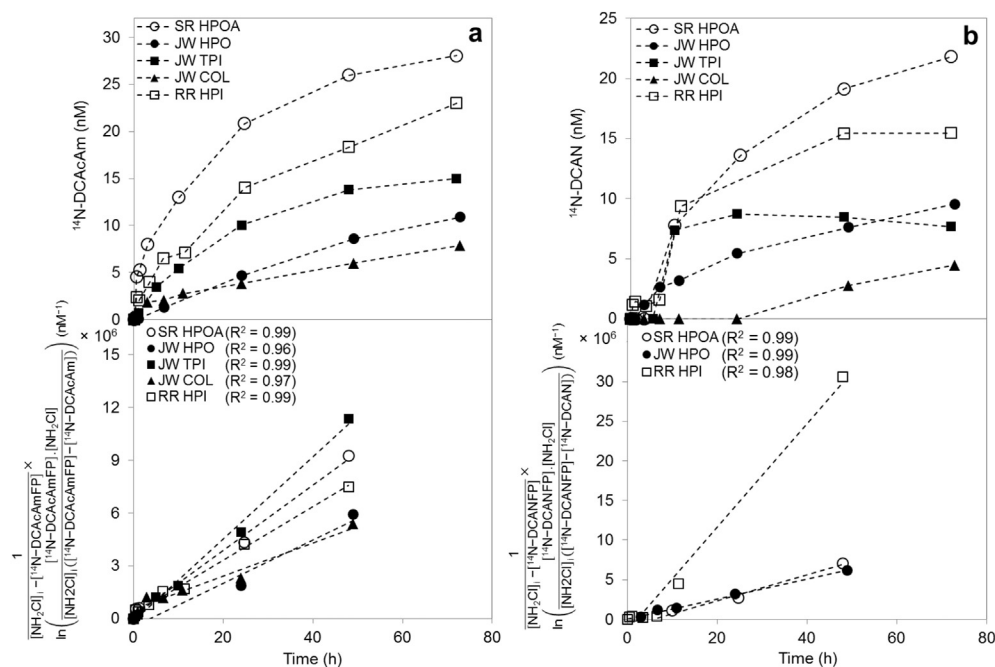


Fig. 2. Formation of a) ^{14}N -DCAcAm and b) ^{14}N -DCAN and their respective second-order relationships for SR HPOA, RR HPI, JW HPO, JW TPI, and JW COL isolates (5 mg C/L) and $^{15}\text{NH}_2\text{Cl}$ (15 mg Cl_2/L) at pH 8 (10 mM phosphate buffer) over 72 h.

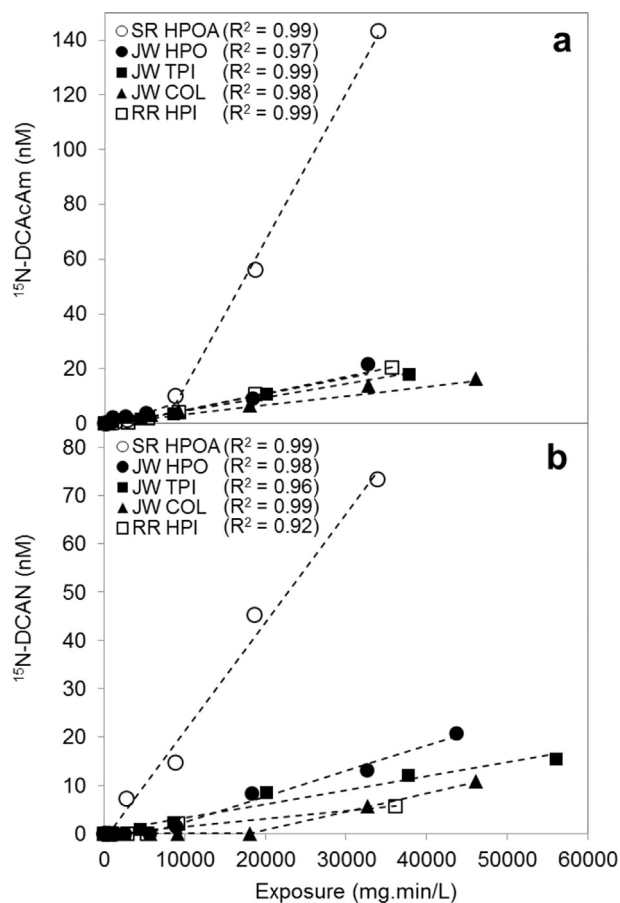


Fig. 3. Formation of a) ^{15}N -DCAcAm and b) ^{15}N -DCAN from SR HPOA, RR HPI, JW HPO, JW TPI, and JW COL isolates (5 mg C/L) and $^{15}\text{NH}_2\text{Cl}$ (15 mg Cl_2/L) at pH 8 (10 mM phosphate buffer) over 72 h.

through the Aldehyde Pathway or indirectly through the hydrolysis of HANs. DCACAl and TCACAl were monitored during the kinetics studies involving ^{15}N - NH_2Cl to compare their formation with HACams formation (Fig. 4). TCACAl was only detected with JW HPO at very low concentrations (7.7 nM at 72 h). DCACAl formation did not fit with any second-order kinetics and a linear correlation with oxidant exposure could not be established. As described in Fig. 4b for JW HPO, the kinetics of formation followed a 2nd order-like profile in the first 10 h of reaction and then linearly increased with monochloramine exposure, reaching a concentration of 28.5 nM after 72 h. Similarly to N-DBPs, DCACAl formation could be attributed to two types of reaction mechanisms: a) a formation from N-org precursors or an intermediate in the first hours of reaction, followed by b) a slow reaction with monochloramine. This second step of formation could be linked to the formation of DCACAl, i.e., the linear increase in DCACAl concentrations would follow the linear formation of DCACAl through the incorporation of a N atom from NH_2Cl and the formation of a carbinolamine (2-dichloro-1-(chloroamino)ethanol) and a N-chloroamide (N-chlorodichloroacetamide) intermediate (Kimura et al., 2013). The formation of N-chlorodichloroacetamide has been reported during chlorination of DCAN at pH 10 (Peters et al., 1990). It was not detected at lower pH values, because N-chloroamides are easily hydrolyzed in the presence of HOCl. Samples from this study were analyzed in full scan mode GC-MS, but no peaks corresponded to the abovementioned intermediates. Despite its two-steps profile, DCACAl formation from JW HPO did not exhibit the same kinetics profile as DCACAm and DCAN formation, since more DCACAl was formed in the first hours of reaction and the linear increase of DCACAm and DCAN was finally more pronounced than that of DCACAl (Fig. S6, SI). A similar observation was made from SR HPOA, which formed the highest DCACAl concentration (43.5 nM at 72 h) but in limited proportions as compared to DCACAm and DCAN. These results indicate that DCACAl formation followed an independent pathway from DCACAm formation. However, additional investigations are needed to confirm this hypothesis.

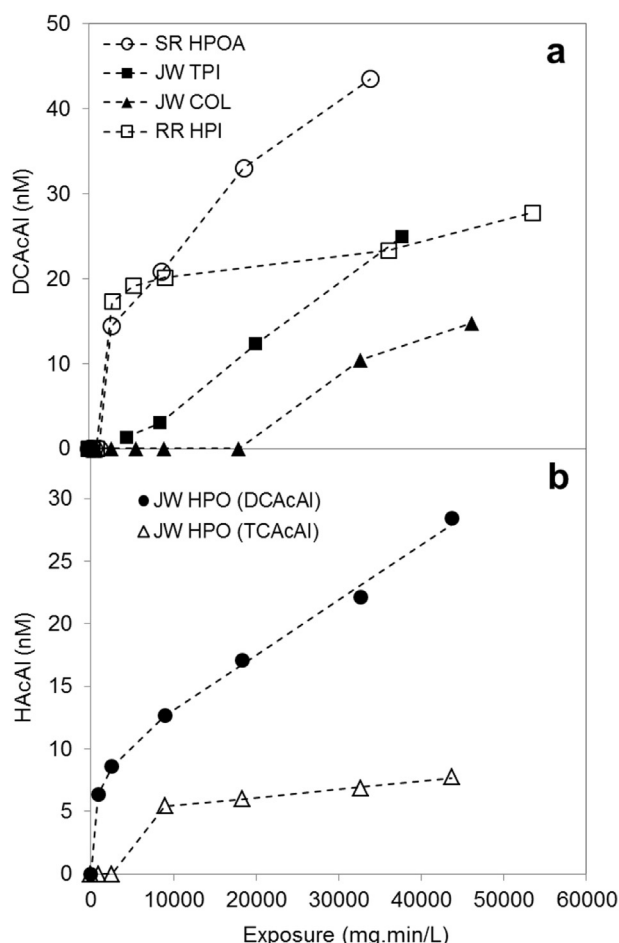


Fig. 4. Formation of a) DCAcAl and b) DCAcAl and TCACAl from SR HPOA, RR HPI, JW HPO, JW TPI, and JW COL isolates (5 mg C/L) and $^{15}\text{NH}_2\text{Cl}$ (15 mg Cl_2/L) at pH 8 (10 mM phosphate buffer) over 72 h.

In contrast to other DBPs, the production of DCAA from SR HPOA exhibited the exact same formation profile as total DCAcAm (i.e., the sum of ^{14}N -DCAcAm and ^{15}N -DCAcAm), and their concentrations were strongly correlated along the reaction time ($R^2 = 0.999$) (Fig. S7, SI). Good fittings were also obtained for other DOM isolates (R^2 ranging from 0.96 to 0.98). DCAA concentrations were approximately two times higher than DCAcAm concentrations for all isolates (i.e., the average slope was 2.1 ± 0.5). This result indicates a direct relationship between the two DBPs during chloramination of DOM, which can be related to the hydrolysis of DCAcAm to DCAA observed during chlorination (Peters et al., 1990; Reckhow et al., 2001).

While the formation of 1,1-DCP mainly occurred from DOM isolates presenting a strong aromatic character (Table S3, SI), its formation did not linearly increase with chloramine exposure and followed second-order kinetics (Fig. S5, SI). This different behavior compared to those of DCAN and DCAcAm indicates that its formation mechanism follows a more complex pathway than the solely incorporation of $^{15}\text{NH}_2\text{Cl}$ in aromatic moieties. Since 1,1-DCP kinetics reached a plateau at reaction times where DCAN and DCAcAm were still linearly increasing, its formation might depend on the availability of an intermediate rather than that of aromatic precursors.

3.3. DBP formation potentials

To verify the hypothesis of the aromatic character of DOM playing a role in the formation of N-DBPs during chloramination, DBP formation potentials from seven DOM isolates were determined after 72 h of chloramination using $^{15}\text{NH}_2\text{Cl}$ at pH 8. As previously observed, major DBP species produced for each class of monitored DBPs (i.e., HAAs, HACams, HACAls) were dichlorinated in the experimental conditions used. Similarly to the kinetics experiments, DCAA was the major DBP analyzed for all the isolates, with concentrations ranging between 56.0 nM (JW COL) and 594.6 nM (BR HPO). DCAA concentrations were higher than TCM concentrations, in accordance with previous studies conducted on the chloramination of natural waters (Hua and Reckhow, 2007). DCAcAm exhibited the highest concentrations after DCAA and TCM, reaching $132 (\pm 76)$ nM for SR HPOA. DCAcAl concentrations were close to those of DCAN, ranging from 14.8 nM (JW COL) to 40.4 nM (SR HPOA). TCAA and TCACAl were also observed at low concentrations (4.0–7.7 nM) (Table S3, SI).

Almost all isolates exhibited a higher proportion of ^{15}N incorporation than ^{14}N , either in DCAcAm or in DCAN (i.e., only RR HPI formed more ^{14}N -DCAN than ^{15}N -DCAN) (Table 1). Similarly to results obtained from kinetics experiments, the highest concentrations of either ^{14}N -DBPs or ^{15}N -DBPs were obtained with SR HPOA. Even if no correlation could be derived from the whole set of results, the general trend was the higher the SUVA of the DOM isolate the higher the incorporation of ^{15}N in N-DBPs (Fig. S8, SI). When discriminating the OM isolates as a function of their origin (i.e., 3 HPO fractions from river waters in one group and 3 fractions from wastewater effluent in another group), good correlations were obtained between ^{15}N -DBPs formation and SUVA values ($R^2 = 0.92$ for ^{15}N -DCAcAm and $R^2 = 0.999$ for ^{15}N -DCAN) (Fig. S8 and Table S4, SI). These results are in good agreement with previous studies which demonstrated that the formation of DCAN during chloramination did not correlate with DON/DOC ratio values of DOM fractions but correlated well with their SUVA values (Yang et al., 2008). In addition to these correlations with SUVA, ^{15}N -DCAcAm and ^{15}N -DCAN formations exhibited a linear relationship against each other ($R^2 = 0.93$, Fig. 5). This observation suggests a similar behavior of DCAcAm and DCAN towards the incorporation of $^{15}\text{NH}_2\text{Cl}$ as SUVA of DOM increases. Such a relationship could not be established from ^{14}N -DCAcAm and ^{14}N -DCAN, suggesting that ^{14}N incorporation did not follow a common pattern for the two species of DBPs. This agrees with results from Huang et al. (2012), who proposed that DCAcAm formation could be independent from DCAN hydrolysis. DCAcAm formation from humic-like materials was proposed to rapidly occur through the Decarboxylation Pathway, followed by the incorporation of inorganic nitrogen through the Aldehyde Pathway becoming more important with

Table 1

Proportion of nitrogen incorporation in DCAN and DCAcAm by chloramination (15 mg Cl_2/L) of OM isolates (DOC = 5 mg C/L) at pH 8 during 72 h of contact time.

Isolate	Concentration (nM) (N incorporation – % ^a)							
	^{14}N -DCAN		^{15}N -DCAN		^{14}N -DCAcAm		^{15}N -DCAcAm	
SR HPOA	19.1	(27)	51.8	(73)	28.0	(21)	104.0	(79)
BR HPO	8.7	(20)	34.1	(80)	13.7	(22)	49.7	(78)
GR HPO	2.0	(12)	14.3	(88)	11.2	(26)	31.5	(74)
RR HPI	11.3	(66)	5.8	(34)	13.9	(44)	17.7	(56)
JW HPO	10.9	(34)	20.7	(66)	2.0	(33)	4.1	(67)
JW TPI	7.7	(33)	15.4	(67)	3.0	(46)	3.5	(54)
JW COL	4.5	(29)	10.8	(71)	11.4	(41)	16.5	(59)

^a N incorporation = nitrogen proportion in N-DBPs, calculated as $\frac{[^{14}\text{N}]\text{NDBP} + [^{15}\text{N}]\text{NDBP}}{([^{14}\text{N}]\text{NDBP} + [^{15}\text{N}]\text{NDBP})} \times 100$ (%).

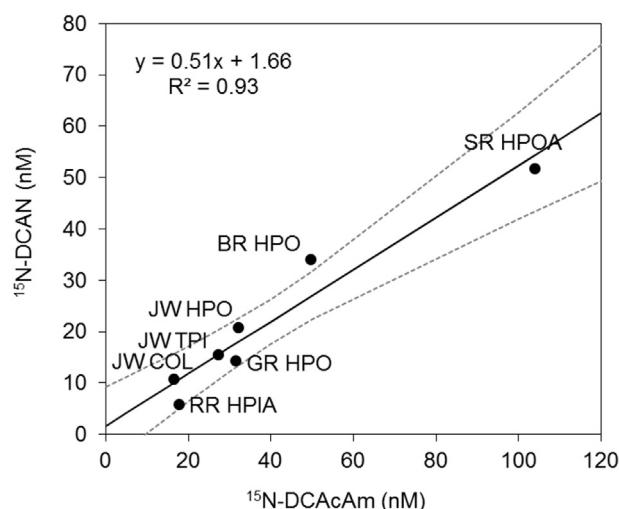


Fig. 5. Relationship between ^{15}N -DCAN and ^{15}N -DCAcAm formation potentials after chloramination ($^{15}\text{NH}_2\text{Cl} = 15 \text{ mg Cl}_2/\text{L}$) of DOM isolates ($\text{DOC} = 5 \text{ mg C/L}$) at pH 8 (10 mM phosphate buffer) during 72 h. Dashed lines represent 95% interval confidence.

increasing chloramines exposure. Thus, DCAN and DCAcAm formation would follow similar but independent pathways during the chloramination of humic substances.

3.4. N-DBP formation potentials from model compounds

Most studies using model precursors for HANs and HACams formation during chlorination and chloramination have focused on amino acids (e.g., asparagine, aspartic acid) (Chu et al., 2012, 2010b; Huang et al., 2012; Trehy et al., 1986; Yang et al., 2010, 2012). Aromatic amino acids (i.e., tryptophan and tyrosine) were demonstrated as important precursors of HACams. A mechanism was recently proposed to describe the formation of TCACAm from the aromatic ring of tyrosine (Chu et al., 2012). Multiple chlorine attacks on the phenolic ring form chloro-, dichloro- and trichlorophenol, ring opening released chloroform, TCAA and a trichloroacetyl chloride (TCAC) intermediate (tentative structure identified by GC–MS). The last step would form TCACAm through TCAC reaction with ammonia and the elimination of hydrochloric acid. However, the mechanism of this critical step, leading to the formation of the amide group (i.e., nitrogen incorporation), is still uncertain. Such a pathway was not described for DCAcAm, which was thought to be formed only from DCAN hydrolysis (Chu et al., 2012). However, DCAcAm was suggested to be formed independently from DCAN hydrolysis during the chloramination of humic substances (Huang et al., 2012). To investigate the reactivity of aromatic compounds with monochloramine, N-DBPs formation tests were conducted by chloramination ($100 \text{ mg Cl}_2/\text{L}$) of $250 \mu\text{M}$ phenol (PHE) and resorcinol (RES) for 72 h at pH 7, and results were compared with amino acids previously described as major precursors of N-DBPs (e.g., tyrosine – TYR, aspartic acid – ASP, tryptophan – TRY) (Fig. 6). Phenol and resorcinol formed higher concentrations of DCAN and DCAcAm than the amino acids, proving that aromatic compounds can be major precursors of N-DBPs as compared to other previously proposed nitrogenous precursors. Phenol produced the highest yield of DCAN (4.43% molar yield), while the highest proportion of DCAcAm was obtained from resorcinol (0.83%). This result can be related to the presence of the second hydroxyl group in meta position, known to activate the aromatic ring for electrophilic substitution by chlorine. While the incorporation of nitrogen from NH_2Cl was

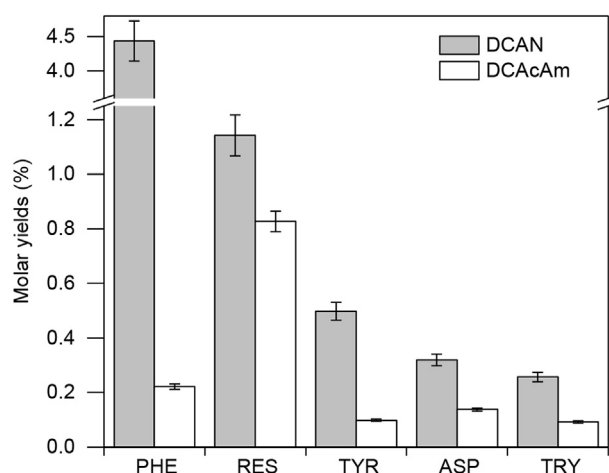


Fig. 6. DCAN and DCAcAm formation by chloramination ($100 \text{ mg Cl}_2/\text{L}$) of phenol, resorcinol, tyrosine, aspartic acid, and tryptophan ($250 \mu\text{M}$) over 72 h and at pH 7 (10 mM phosphate buffer). Molar yields were calculated based upon the initial model precursor concentration. Error bars represent standard deviations ($n = 3$). PHE: phenol; RES: resorcinol; TYR: tyrosine; ASP: aspartic acid; TRY: tryptophan.

previously hypothesized to occur through the Aldehyde Pathway (Huang et al., 2012), these results show that aromatic organic compounds react with monochloramine to produce N-DBPs through an unknown mechanism.

4. Conclusions

This study demonstrates the possibility of N-DBPs formation from aromatic moieties of DOM. Experiments using aromatic model compounds confirm the results obtained from DOM isolates. The results from this investigation are of significant importance for water treatment facilities using chloramines as final disinfectant, where the removal of aromatic DOC must be optimized to avoid the production of N-DBPs. This work also confirms the possibility of two distinct mechanisms explaining N-DBP formation during chlorination/chloramination of aromatic amino acids, i.e., chlorination of amino groups and incorporation of inorganic nitrogen from NH_2Cl in aromatic rings. The mechanism of N-DBPs formation through aromatic ring opening and nitrogen incorporation requires further investigation to be elucidated. Kinetics experiments and structural identifications of potential reaction intermediates should be performed in order to understand this pathway. Potential intermediates include carbinolamines and N-chloroamides, both previously observed as intermediates during the chloramination of aldehydes and the chlorination of acetamides, respectively.

Acknowledgments

Research reported in this publication was supported by the King Abdullah University of Science and Technology (KAUST). The authors would also like to thank Dr. Leo Gutierrez for his assistance and support.

Appendix A. Supplementary data

Supplementary data related to this article can be found at <http://dx.doi.org/10.1016/j.watres.2015.10.036>.

References

- Bond, T., Henriot, O., Goslan, E.H., Parsons, S.A., Jefferson, B., 2009. Disinfection byproduct formation and fractionation behavior of natural organic matter

- surrogates. *Environ. Sci. Technol.* 43, 5982–5989.
- Bond, T., Huang, J., Templeton, M.R., Graham, N., 2011. Occurrence and control of nitrogenous disinfection by-products in drinking water – a review. *Water Res.* 45, 4341–4354.
- Bond, T., Templeton, M.R., Graham, N., 2012. Precursors of nitrogenous disinfection by-products in drinking water—A critical review and analysis. *J. Hazard. Mater.* 235–236, 1–16.
- Chuang, Y.-H., Lin, A.Y.-C., Wang, X., Tung, H., 2013. The contribution of dissolved organic nitrogen and chloramines to nitrogenous disinfection byproduct formation from natural organic matter. *Water Res.* 47, 1308–1316.
- Chuang, Y.-H., Tung, H., 2015. Formation of trichloronitromethane and dichloroacetonitrile in natural waters: precursor characterization, kinetics and interpretation. *J. Hazard. Mater.* 283, 218–226.
- Chu, W., Gao, N., Deng, Y., 2010a. Formation of haloacetamides during chlorination of dissolved organic nitrogen aspartic acid. *J. Hazard. Mater.* 173, 82–86.
- Chu, W., Gao, N., Krasner, S.W., Templeton, M.R., Yin, D., 2012. Formation of halogenated C-, N-DBPs from chlor(am)ination and UV irradiation of tyrosine in drinking water. *Environ. Pollut.* 161, 8–14.
- Chu, W., Gao, N.-Y., Deng, Y., 2010b. Precursors of dichloroacetamide, an emerging nitrogenous DBP formed during chlorination or chloramination. *Environ. Sci. Technol.* 44, 3908–3912.
- Chu, W., Gao, N., Yin, D., Krasner, S.W., 2013. Formation and speciation of nine haloacetamides, an emerging class of nitrogenous DBPs, during chlorination or chloramination. *J. Hazard. Mater.* 260, 806–812.
- Croué, J.-P., 2004. Isolation of humic and non-humic NOM fractions: structural characterization. *Environ. Monit. Assess.* 92, 193–207.
- Dotson, A., Westerhoff, P., Krasner, S.W., 2009. Nitrogen enriched dissolved organic matter (DOM) isolates and their affinity to form emerging disinfection by-products. *Water Sci. Technol.* 60, 135–143.
- Drewes, J.E., Croué, J.-P., 2002. New approaches for structural characterization of organic matter in drinking water and wastewater effluents. *Water Sci. Technol. Water Supply* 2, 1–10.
- Eaton, A.D., Clesceri, L.S., Greenberg, A.E. (Eds.), 1995. *Standard Methods for the Examination of Water and Wastewater*, nineteenth ed. American Public Health Association/American Water Works Association/Water Environment Federation Publishers, Washington D.C., USA.
- Fang, J., Ma, J., Yang, X., Shang, C., 2010. Formation of carbonaceous and nitrogenous disinfection by-products from the chlorination of *Microcystis aeruginosa*. *Water Res.* 44, 1934–1940.
- Glezer, V., Harris, B., Tal, N., Josefzon, B., Lev, O., 1999. Hydrolysis of haloacetonitriles: linear free energy relationship. Kinetics and products. *Water Res.* 33, 1938–1948.
- Gonsior, M., Zwartjes, M., Cooper, W.J., Song, W., Ishida, K.P., Tseng, L.Y., Jeung, M.K., Rosso, D., Hertkorn, N., Schmitt-Kopplin, P., 2011. Molecular characterization of effluent organic matter identified by ultrahigh resolution mass spectrometry. *Water Res.* 45, 2943–2953.
- Hua, G., Reckhow, D.A., 2007. Comparison of disinfection byproduct formation from chlorine and alternative disinfectants. *Water Res.* 41, 1667–1678.
- Huang, H., Wu, Q.-Y., Hu, H.-Y., Mitch, W.A., 2012. Dichloroacetonitrile and dichloroacetamide can form independently during chlorination and chloramination of drinking waters, model organic matters, and wastewater effluents. *Environ. Sci. Technol.* 46, 10624–10631.
- Huang, H., Wu, Q.-Y., Tang, X., Jiang, R., Hu, H.-Y., 2013. Formation of haloacetonitriles and haloacetamides during chlorination of pure culture bacteria. *Chemosphere* 92, 375–381.
- Jafvert, C.T., Valentine, R.L., 1992. Reaction scheme for the chlorination of ammoniacal water. *Environ. Sci. Technol.* 26, 577–786.
- Kimura, S.Y., Komaki, Y., Plewa, M.J., Mariñas, B.J., 2013. Chloroacetonitrile and N,2-dichloroacetamide formation from the reaction of chloroacetaldehyde and monochloramine in water. *Environ. Sci. Technol.* 47, 12382–12390.
- Krasner, S.W., Scilimenti, M.J., Mitch, W., Westerhoff, P., Dotson, A., 2007. Using formation potential tests to elucidate the reactivity of DBP precursors with chlorine versus with chloramines. In: *Proceedings of the 2007 AWWA Water Quality Technology Conference*. AWWA, Denver.
- Krasner, S.W., Weinberg, H.S., Richardson, S.D., Pastor, S.J., Chinn, R., Scilimenti, M.J., Onstad, G.D., Thruston Jr., A.D., 2006. Occurrence of a new generation of disinfection byproducts. *Environ. Sci. Technol.* 40, 7175–7185.
- Leenheer, J.A., Croué, J.P., 2003. Characterizing aquatic dissolved organic matter. *Environ. Sci. Technol.* 37, 18A–26A.
- Leenheer, J.A., Croué, J.P., Benjamin, M., Korshin, G.V., Hwang, C.J., Bruchet, A., Aiken, G.R., 2000. Comprehensive isolation of natural organic matter from water for spectral characterizations and reactivity testing. In: *Natural Organic Matter and Disinfection By-products*, ACS Symposium Series. American Chemical Society, pp. 68–83.
- Mitch, W.A., Sedlak, D.L., 2004. Characterization and fate of n-nitrosodimethylamine precursors in municipal wastewater treatment plants. *Environ. Sci. Technol.* 38, 1445–1454.
- Muellner, M.G., Wagner, E.D., Mccalla, K., Richardson, S.D., Woo, Y.-T., Plewa, M.J., 2007. Haloacetonitriles vs. regulated haloacetic acids: are nitrogen-containing DBPs more toxic? *Environ. Sci. Technol.* 41, 645–651.
- Munch, D.J., Hautman, D.P., 1995. EPA Method 551.1 Determination of Chlorination Disinfection Byproducts, Chlorinated Solvents, and Halogenated Pesticides/Herbicides in Drinking Water by Liquid-liquid Extraction and Gas Chromatography with Electron-capture Detection, Revision 1.0. United States Environmental Protection Agency, Cincinnati, OH.
- Munch, D.J., Munch, J.W., 1995. EPA Method 552.2 Determination of Haloacetic Acids and Dalapon in Drinking Water by Liquid-liquid Extraction, Derivatization and Gas Chromatography with Electron Capture Detection, Revision 1.0. United States Environmental Protection Agency, Cincinnati, OH.
- Oliver, B.G., 1983. Dihaloacetonitriles in drinking water: algae and fulvic acid as precursors. *Environ. Sci. Technol.* 17, 80–83.
- Pedersen, E.J., Urbansky, E.T., Marinas, B.J., Margerum, D.W., 1999. Formation of cyanogen chloride from the reaction of monochloramine with formaldehyde. *Environ. Sci. Technol.* 33, 4239–4249.
- Peters, R.J.B., De Leer, W.B.E., De Galan, L., 1990. Chlorination of cyanoethanoic acid in aqueous medium. *Environ. Sci. Technol.* 24, 81–86.
- Plewa, M.J., Wagner, E.D., Jazwierska, P., Richardson, S.D., Chen, P.H., McKague, A.B., 2004. Halonitromethane drinking water disinfection byproducts: chemical characterization and mammalian cell cytotoxicity and genotoxicity. *Environ. Sci. Technol.* 38, 62–68.
- Plewa, M.J., Wagner, E.D., Muellner, M.G., Hsu, K.-M., Richardson, S.D., 2008. Comparative mammalian cell toxicity of n-DBPs and c-DBPs. In: *Disinfection By-products in Drinking Water*, ACS Symposium Series. American Chemical Society, pp. 36–50.
- Reckhow, D.A., MacNeill, A.L., Platt, T.L., MacNeill, A.L., McClellan, J.N., 2001. Formation and degradation of dichloroacetonitrile in drinking waters. *J. Water Supply Res. Technol.* – AQUA 50, 1–13.
- Reckhow, D.A., Singer, P.C., 1985. Mechanisms of organic halide formation during fulvic acid chlorination and implications with respect to preozonation. In: Jolley, R.L. (Ed.), *Water Chlorination Chemistry: Environmental Impact and Health Effects*. Ann Arbor Science Publishers, p. 1229.
- Reckhow, D.A., Singer, P.C., Malcolm, R.L., 1990. Chlorination of humic materials: byproduct formation and chemical interpretations. *Environ. Sci. Technol.* 24, 1655–1664.
- Schreiber, I.M., Mitch, W.A., 2005. Influence of the order of reagent addition on NDMA formation during chloramination. *Environ. Sci. Technol.* 39, 3811–3818.
- Suffet, I.H., Brenner, L., Silver, B., 1976. Identification of 1,1,1-trichloroacetone (1,1,1-trichloropropanone) in two drinking waters: a known precursor in haloform reaction. *Environ. Sci. Technol.* 10, 1273–1275.
- Trehy, M.L., Yost, R.A., Miles, C.J., 1986. Chlorination byproducts of amino acids in natural waters. *Environ. Sci. Technol.* 20, 1117–1122.
- Weinberg, H.S., Krasner, S.W., Richardson, S.D., Thruston Jr., A.D., 2002. The occurrence of disinfection by-products (DBPs) of health concern in drinking water: results of a Nationwide DBP occurrence study. EPA/600/R02/068.
- Westerhoff, P., Mash, H., 2002. Dissolved organic nitrogen in drinking water supplies: a review. *J. Water Supply Res. Technol.* – AQUA 51, 415–448.
- Yang, X., Fan, C., Shang, C., Zhao, Q., 2010. Nitrogenous disinfection byproducts formation and nitrogen origin exploration during chloramination of nitrogenous organic compounds. *Water Res.* 44, 2691–2702.
- Yang, X., Guo, W., Shen, Q., 2011. Formation of disinfection byproducts from chlor(am)ination of algal organic matter. *J. Hazard. Mater.* 197, 378–388.
- Yang, X., Shang, C., Lee, W., Westerhoff, P., Fan, C., 2008. Correlations between organic matter properties and DBP formation during chloramination. *Water Res.* 42, 2329–2339.
- Yang, X., Shang, C., Westerhoff, P., 2007. Factors affecting formation of haloacetonitriles, halo ketones, chloropicrin and cyanogen halides during chloramination. *Water Res.* 41, 1193–1200.
- Yang, X., Shen, Q., Guo, W., Peng, J., Liang, Y., 2012. Precursors and nitrogen origins of trichloronitromethane and dichloroacetonitrile during chlorination/chloramination. *Chemosphere* 88, 25–32.